Ammonia independent sodium uptake mediated by Na^+ channels and NHEs in the freshwater ribbon leech *Nephelopsis obscura*

Alex R. Quijada-Rodriguez[1], Aaron G. Schultz[2], Jonathan M. Wilson[3], Yuhe He[4], Garett J.P. Allen[1], Greg G. Goss[4], Dirk Weihrauch[1*]

* Corresponding author (email: Dirk.weihrauch@umanitoba.ca), [1]Department of Biological Sciences, University of Manitoba, Winnipeg, MB R3T2N2, Canada; [2]School of Life and Environmental Sciences, Deakin University, Geelong, Australia. Locked Bag 20000, Geelong, VIC 3220, Australia; [3]Department of Biology, Wilfrid Laurier University, Waterloo ON, Canada N2L 3C5; [4] Department of Biological Sciences, University of Alberta, Edmonton, T6G 2E9, Canada

Address for correspondence: Department of Biological Sciences, University of Manitoba, 190 Dysart Road, Winnipeg, MB R3T2N2, Canada

Keywords: Rh-NHE metabolon, Rh proteins, H^+-ATPase, ammonia excretion, freshwater, osmoregulation

Journal of Experimental Biology • Advance article

Abstract

Freshwater organisms actively take up ions from their environment to counter diffusive ion losses due to inhabiting hypo-osmotic environments. The mechanisms behind active Na^+ uptake are quite well understood in freshwater teleosts, however, the mechanisms employed by invertebrates are not. Pharmacological and molecular approaches were used to investigate Na^+ uptake mechanisms and their link to ammonia excretion in the ribbon leech *Nephelopsis obscura*. At the molecular level, we identified a Na^+ channel and a Na^+/H^+-exchanger (NHE) in the skin of *N. obscura*, where the NHE was upregulated when acclimated to extremely low $[Na^+]$ (0.05 mmol l^{-1}, pH 5) conditions. Additionally, we found that leeches in dilute freshwater environments use both, a vacuolar-type H^+-ATPase (VHA) assisted uptake *via* a Na^+ channel and a NHE based mechanisms for Na^+ uptake. Immunolocalization of VHA and Na^+/K^+ ATPase indicated at least two cell types present within leech skin, VHA^+ and VHA^- cells, where the VHA^+ cells are likely involved in Na^+ uptake. NKA was present throughout the epithelium. We also found that increasing ammonia excretion by decreasing water pH, ammonia loading leeches or exposing leeches to high environmental ammonia does not affect Na^+ uptake providing indications that an NHE-Rh metabolon is not present and that ammonia excretion and Na^+ uptake are not coupled in *N. obscura*. To our knowledge, this is the first study showing the mechanisms of Na^+ uptake and their links to ammonia excretion in a freshwater invertebrate, where results suggest an ammonia-independent Na^+ uptake mechanism relying on both Na^+ channels and NHEs.

1. Introduction

Freshwater environments are characteristically hypo-osmotic relative to the internal fluids of their inhabitants and thus innately challenge ion homeostasis of freshwater organisms through a passive ion loss and water gain. With Na^+ and Cl^- composing the majority of ions within the extracellular fluids, tight regulation of these two ions is essential. Freshwater organisms have evolved several mechanisms to counteract ion loss and osmotic water gain; these mechanisms include production of hypo-osmotic urine, reduction of ion permeability through tight epithelia, and active NaCl uptake mechanisms (Larsen et al., 2014; Quijada-Rodriguez et al., 2017). Generally, the basolaterally localized Na^+/K^+ ATPase (NKA) is a major driving force for active Na^+ uptake in the osmoregulatory active tissues of freshwater organisms, such as gills and skin (Larsen et al., 2014). The majority of research investigating Na^+ transport mechanisms in freshwater have mainly focused on teleost fishes. In fishes, a number of putative Na^+ transport mechanisms have been proposed including H^+-ATPase (generating a strong negative cell potential) assisted Na^+ uptake through Na^+ channels, electroneutral exchange of Na^+ for H^+ or NH_4^+ through electroneutral Na^+/H^+ exchangers (NHE), and most recently, Cl^- linked Na^+ uptake through Na^+/Cl^- cotransporters (NCC) (Dymowska et al., 2012; Hwang, 2009; Kumai and Perry, 2012; Parks et al., 2008). With multiple transport mechanisms having been proposed in freshwater teleosts, the feasibility of the aforementioned Na^+ uptake mechanisms to function under freshwater conditions have been the subject of constant debate with numerous studies providing evidence for or refuting these apical Na^+ uptake mechanisms.

Na^+/H^+ exchangers (NHE) have received considerable attention as potential key transporters involved in the Na^+ uptake of freshwater organisms. However, as electroneutral NHE function is solely dependent on Na^+ and H^+ concentration gradients, the viability of NHEs for Na^+ uptake in freshwater has been challenged based on thermodynamic constraints

(Avella and Bornancin, 1989; Parks et al., 2008). Arguably the most critical study supporting NHE function in freshwater is the characterization of NHE3 in the Osorezan dace, *Tribolodon hakonensis* (Hirata et al., 2003). Here, NHE3 was localized to the apical membrane of the gills, upregulated when transferred to low pH, and was functionally characterized in *Xenopus* oocytes (Hirata et al., 2003). What makes these findings extraordinary is that the Osorezan dace inhabits a low Na^+ and extremely acidic (pH 3.5) freshwater environment; an environment, which should be, theoretically, highly unfavorable for proper NHE function. Since the study on the Osorezan dace, numerous other studies have provided physiological and molecular evidence supporting the role of NHEs in freshwater. Cumulative physiological and molecular data has made it evident that NHEs function in freshwater despite thermodynamic constraints (Boyle et al., 2016; Brix et al., 2015; Edwards et al., 1999; Inokuchi et al., 2009; Ivanis et al., 2008; Kumai and Perry, 2011; Shih et al., 2012; Wilson et al., 2000; Wu et al., 2010; Yan et al., 2007).

One explanation for NHEs functioning in freshwater could be an NHE-Rh metabolon hypothesized by Wright and Wood (2009), where a localized alkalization is created on the apical surface of mitochondria-rich cells (MRCs) by NH_3 excretion *via* Rhesus glycoproteins. This alkalization would essentially generate a H^+ gradient driving Na^+/H^+ exchange by NHEs thus linking Na^+ uptake to ammonia excretion. The NHE-Rh metabolon has been supported, for instance, through scanning ion-selective electrode technique (SIET) that demonstrated a localized alkalization, increased ammonia excretion, and increased Na^+ uptake at the apical surface of MRCs in the skin of medaka (*Oryzias latipes*) larvae where NHE3 was colocalized with Rhcg1 and where both became upregulated in the presence of low Na^+ (Wu et al., 2010). While the NHE-Rh metabolon may explain how NHEs overcome thermodynamic constraints in particularly acidic freshwaters, it is likely an ineffective solution to achieve proper NHE function in extremely low Na^+ (<0.05 mmol l^{-1}) environments (Dymowska et al., 2012).

As an alternative to NHEs, Avella and Bornancin (1989) proposed the VHA mediated Na^+ channel mechanism for Na^+ absorption by which an apical vacuolar-type H^+-ATPase (VHA) causes an intracellular hyper-polarization driving Na^+ uptake *via* Na^+ channels. Through immunofluorescence, Wilson et al. (2000) initially co-localized a VHA and a presumably epithelial Na^+ channel (ENaC) to the apical membrane of pavement cells and MRCs of rainbow trout gills. While identified with human ENaC antibodies in rainbow trout gills, an ENaC sequence has yet to be identified in any fish genome challenging the validity of VHA mediated Na^+ channel mechanism. Nevertheless, the dependence of Na^+ uptake on VHA is apparent from numerous pharmacological, knockdown, and molecular studies (Esaki et al., 2007; Fenwick et al., 1999; Horng et al., 2007; Kumai and Perry, 2011; Yan et al., 2007). Although the role of VHA remained relatively clear in Na^+ uptake, a candidate Na^+ channel remained unidentified until the recent characterization of acid sensing ion channels (ASIC) as a Na^+ transporter localized to the apical membrane of H^+-ATPase rich cells and MRCs in zebrafish and trout gills, respectively (Dymowska et al., 2014; Dymowska et al., 2015). Taken together, the identification of ASICs as Na^+ transporters and evidence supporting the role of V-ATPase in Na^+ uptake provide strong evidence for the VHA mediated Na^+ channel mechanism initially proposed by Avella and Bornancin (1989).

Compared to freshwater fishes, Na^+ uptake mechanisms remain poorly understood amongst freshwater invertebrates. The present study focuses on the ribbon leech *Nephelopsis obscura*, which inhabits freshwater systems throughout Canada and the Northern United States (Davies, 1973), where freshwater Na^+ concentrations are quite variable ranging from 0.02 mmol l^{-1} (e.g. Vancouver, BC, Canada) to 2 mmol l^{-1} (e.g. Winnipeg, MB, Canada) (see Genz et al., 2013; Parks et al., 2008). Although to date not studied in *N. obscura*, early physiological studies on isolated freshwater leech skin preparations (*Hirudo medicinalis*) have previously demonstrated the active Na^+ uptake capability of this epithelia (Weber et al.,

1993). Further, leech skin has also been identified as a major site of ammonia excretion and, at least in *N. obscura*, appears to express a number of key transporters involved in Na^+ uptake, including Na^+/K^+-ATPase (NKA), a Rhesus protein (Rh protein), and vacuolar-type H^+-ATPase (VHA) (Quijada-Rodriguez et al., 2017; Quijada-Rodriguez et al., 2015). The Na^+ and ammonia transport capabilities of leech skin combined with the known expression of the aforementioned transporters suggests the possibility of two Na^+ uptake mechanisms commonly observed in freshwater fish, a VHA mediated uptake via a Na^+ channel and uptake *via* an apical NHE. However, to date, these mechanisms have never been identified in leech skin.

Given varying theories on apical Na^+ transport mechanisms in freshwater organisms and a current void of knowledge on the subject, particularly amongst freshwater invertebrates, this study aims to further knowledge of Na^+ uptake mechanisms in freshwater invertebrates by identifying the mechanism of cutaneous Na^+ uptake in the *N. obscura* through radiolabeled ^{22}Na fluxes. Further, given the NHE-Rh metabolon hypothesis has proposed a linkage between Na^+ uptake and ammonia excretion in freshwater organisms, we also tested this hypothesis by simultaneous measurements of ^{22}Na and ammonia flux in the presence of various pharmacological agents and under environmental conditions known to influence ammonia excretion.

2. Methods

2.1 Animals

Leeches *(N. obscura)* were obtained from Manny's Live Bait (Winnipeg, MB). Leeches were transferred to the University of Alberta (Edmonton, AB) for flux experiments and maintained in flow through 37 L aquariums containing aerated dechlorinated Edmonton tap water (ETW, 12°C, pH ~8, Na^+ ~0.45 mmol l^{-1}) with a 14h light/10h dark photoperiod and

fed frozen bloodworms *ad libitum* once a week. All experiments were performed at 12°C on leeches starved for a minimum of seven days to prevent skewed flux rates due to elevated amino acid metabolism. For low ionic strength water experiments (artificially made freshwater containing Na^+ = 0.05 mmol l^{-1}, Cl^- = 0.075 mmol l^{-1}, Ca^{2+} = 0.025 mmol l^{-1}, pH 5), leeches were acclimated for 4 days in 10 L aquariums and maintained at 12°C with constant aeration.

2.2 Whole animal flux experiments

In whole animal flux experiments, three experimental series were used. The first experimental series investigated the effect of pharmacological agents on Na^+ and ammonia fluxes in ETW. In the second experimental series, the effects of low ionic strength water acclimation on Na^+ and ammonia fluxes were investigated. In the third experimental series the effect of altered ammonia excretion through environmental manipulation (e.g. pH and environmental ammonia) on Na^+ uptake was determined. Isolated leech skin preparations were avoided in this study to assure *in vivo* Na^+ and ammonia gradients were present during all flux experiments. For experiments where pH was adjusted, NaOH or HCl were used to adjusted pH.

In all three experimental series, individual leeches were placed into sealed 60 ml chambers containing 40 ml of ETW or low ionic strength water and constantly aerated. Prior to flux experiments, leeches were given an initial one-hour acclimation period in the experimental chambers. Following the acclimation period, chamber water was refreshed prior to beginning flux experiments. During flux experiments where leeches were exposed to ETW enriched with either high ammonia concentrations or varying environmental pH regimes, the adjusted media was added to the experimental chamber post-acclimation period.

Unidirectional Na$^+$ (using radiolabeled ^{22}Na) and ammonia fluxes were measured over a two hour flux period adapted from previously established protocols (Goss and Wood, 1990). In brief, 0.1 μCi l^{-1} ^{22}Na was added to each experimental chamber and mixed for 5 minutes by aeration. For pharmacological experiments, following the addition of ^{22}Na, DMSO (0.05%, control) or pharmacological agents dissolved in DMSO (0.05%) were added to the experimental chambers and mixed for 5 minutes. After mixing, 6.5 ml of chamber water was sampled at time 0 and 2 hours for determination of ^{22}Na radioactivity, total Na$^+$ and ammonia concentration. After the two-hour flux period leeches were blotted dry and weighed.

In the first experimental series, various ENaC, ASIC, NHE, and VHA inhibitors were employed to determine the role of these transporters in Na$^+$ and ammonia flux. To determine the optimal inhibitory concentrations for amiloride, a non-specific Na$^+$ channel and NHE inhibitor, and 5-(N-ethyl-N-isopropyl)amiloride (EIPA), an NHE specific inhibitor (Kleyman and Cragoe, 1988), dose response Na$^+$ and ammonia flux experiments were performed as described above. For phenamil, an ENaC and ASIC inhibitor, and DAPI, an ASIC specific inhibitor (Chen et al., 2010), inhibitory concentrations of 50 and 1 μmol l^{-1} were used based on previous studies of rainbow trout, respectively (Dymowska et al., 2014). Furthermore, based on preliminary experiments using the VHA specific inhibitor, KM91104 (Kartner et al., 2010), a concentration of 10 μmol l^{-1} was used as this was found to have the same inhibitory response as 20 μmol l^{-1}, which was shown to effectively inhibit the VHA in perfused crustaceans gills (Fehsenfeld and Weihrauch, 2016).

Given that extremely low Na$^+$ environments are thermodynamically unfavourable for successful electroneutral NHE function (i.e. Na$^+$ uptake and H$^+$ excretion; Parks et al., 2008), leeches were acclimated to low ionic strength water (0.05 mmol l^{-1} Na$^+$) in the second experimental series. Pharmacological agents employed in experimental series one were

similarly employed in experimental series two to determine if changes in Na^+ uptake mechanisms occur when leeches are acclimated to low ionic strength water.

In the third experimental series, high environmental ammonia (HEA, 1 mmol l^{-1}, pH 8), varying pH, and ammonia loading were used to disrupt ammonia excretion and determine its impact on epithelial Na^+ uptake. These challenges to nitrogen physiology have been shown previously to alter whole animal ammonia excretion in *N. obscura* (Quijada-Rodriguez et al., 2015). In varying pH and HEA experiments, water with adjusted pH or enriched with NH_4Cl was added to experimental chambers following the acclimation period (see above). For post-HEA experiments, NH_4Cl enriched water was added to the chamber during the acclimation period (one hour) and replaced with ammonia free water for the flux period.

2.3 Ammonia and Na^+ analysis

Total water ammonia was measured colourimetrically using a microplate spectrophotometer (Spectramax 190, Molecular Devices) using the salicylate-hypochlorite assay at 595 nm as described by Verdouw and colleagues (1977). For all ammonia assays, a minimum R^2 value of 0.98 was required for standard curve validation. Total Na^+ concentrations were measured by atomic absorption spectrophotometry (model 3300, Perkin Elmer, Shelton, CT) and ^{22}Na radioactivity was measured with a gamma counter (Packard Cobra II, Auto Gamma, model 5010, Perkin Elmer).

Ammonia excretion rates were calculated according to equation 1 where C_{Amm} is the change in ammonia concentration of ammonia between time 0 and 2 hours in nmol l^{-1}, V is the volume during the flux period in litres, t is the flux time in hours, and M is the fresh weight of the leech in grams. Unidirectional ^{22}Na uptake rates were calculated according to equation 2 where ΔCPM is the change in water radioactivity (cpm/ml) between time 0 and 2 hours, V is the flux period volume in ml, SA is the average specific activity (CPM/nmol Na^+)

at the beginning and end of the flux period, t is the flux time in hours and M is the fresh weight of the leech in grams.

$$equation \quad (1) \quad J_{Amm} = \frac{C_{Amm} \times V}{t \times M}$$

$$equation \quad (2) \quad J_{Na^+} = \frac{\Delta CPM \times V}{SA \times t \times M}$$

2.4 Immunohistochemistry

Leeches were immersion fixed whole in either 4% paraformaldehyde in phosphate buffered saline (pH 7.4) at 4°C or 20% dimethylsulfoxide/methanol (DMSO/MeOH) at -20°C. Animals were then processed for paraffin embedding (Richard Allen type 6, Fisher-Thermo), sectioned (5 µm) and sections collected onto APS (aminopropylsilane, Sigma-Aldrich) coated slides for immunohistochemistry (IHC). IHC was performed using indirect fluorescence labelling with antigen retrieval as described by Wilson et al. (2007). In short, successful staining was achieved with 20% DMSO/MeOH fixed tissue with 1% SDS/PBS antigen retrieval for 5 min at room temperature. After rinsing and blocking, sections were incubated overnight at 4°C with either rabbit polyclonal NKA (1:500; Wilson et al., 2007)) or VHA (1:200; Santa Cruz Biotech) antibodies in BLØK buffer (Millipore) or normal rabbit serum as a negative control. The secondary antibody was a goat-rabbit IgG conjugated to Alexa 488 (1:500; Jackson Immunochemicals). Sections were counter stained with DAPI and mounted with 1:1 PBS: glycerol. Images were collected with a Leica DM5500B wide-field epifluorescence microscope and Hamamatsu OrcaFlash 4.0 camera using Leica LASX software.

2.5 Quantitative PCR (qPCR)

Total RNA from leech skin was obtained, purified and reverse transcribed into cDNA as previously described (Quijada-Rodriguez et al., 2015). Synthesized cDNA (from 0.75 µg

Total RNA) quality was evaluated by PCR using the primer pair NoRPS2 F1/R1 (Table 1). All PCR products were assessed by ethidium bromide stained TAE agarose gel electrophoresis.

Partial sequences for the *Nephelopsis obscura* Na$^+$/H$^+$ exchanger (*NoNHE3*) and amiloride sensitive Na$^+$ channel (*NoNaC*) were obtained through degenerate primers. Degenerate primers targeting the Na$^+$/H$^+$ exchanger (DegNHE3 F1/R1) and Na$^+$ channel (DegNaC F1/R1) (Table 1) were designed based on conserved regions of nucleotide sequences of Na$^+$/H$^+$ exchanger 3 and Na$^+$ channel like genes in the leech *Helobdella robusta* genome (DOE Joint Genome Institute). PCR products of the predicted size were purified (E.N.Z.A Gel extraction kit, Bio Tek, Winooski, VT, USA) and sequenced (Robarts Research Institute, London, Ontario, Canada). A GenBank search with BLAST and alignment with corresponding *H. robusta* gene confirmed the identity of the isolated PCR products. For the Na$^+$ channel, a 5' RACE (FirstChoice RLM-RACE Kit, Ambion) was performed employing the NoNaC RACE R1 primer and 5' RLM-RACE kit 5' outer primer forward primer. Obtained PCR fragments were purified, sequenced, and amplicon identified as described above.

Quantitative PCR (qPCR) was performed using an ABI 7500 Real-Time PCR System in 96-well PCR plates (Applied Biosystems, CA). A PCR reaction mixture for one well contained 5 μl of SYBR Green master mix (Applied Biosystems), 2.5 μl of sense/antisense gene-specific primers to final concentrations of 400 nmol l^{-1} (Integrated DNA Technologies, IA), and 2.5 μl of cDNA that was diluted in RNase-free water (Qiagen, Venlo, Netherlands). The PCR thermal cycles were initiated by 2 min denaturation at 95 °C followed by 40 cycles with denaturing for 15 s at 95 °C and annealing and extension for 1 min at 60 °C. Dissociation curve analysis was performed after amplification reactions to ensure single product amplification. Efficiency, uniformity, and linear dynamic range of each qPCR assay

were assessed by construction of standard curves using serially diluted cDNA standards. Four genes including amiloride-sensitive Na$^+$ channel (*NoNac*), Na$^+$/H$^+$ exchanger 3 like (*NoNHE3*), Rhesus glycoprotein (*NoRhp*), and V-type H$^+$-ATPase subunit B (*NoVHA*) were selected for measurement. All primers were designed based on the sequences available in the NCBI GeneBank database or the sequences obtained in the current study. Changes in abundance of transcripts of target genes were quantified using the ΔΔCt method by normalizing to *NoRPS2* (F2/R2 primers, see table 2). Sequences of nucleotide primers used in qPCR are provided in Table 2.

2.5 Chemicals

KM91104 and 5-(N-ethyl-N-isopropyl)amiloride (EIPA) were purchased from Cayman Chemicals (Ann-Arbor, MI, USA). All other chemicals (unless otherwise stated) were of analytical grade and purchased from Sigma-Aldrich (St. Louis, MO, USA).

2.6 Statistics

Data are presented as mean ± standard error (s.e.m.). To determine whether data sets met parametric assumptions, data were tested for homogeneity of variance with Levene's test and normal distribution with Shapiro-Wilk test. Non-parametric analysis for differences between two means was done with Mann-Whitney's U test. Differences between more than two means were tested using a one-way ANOVA with *post-hoc* Tukey's pairwise comparison or *post-hoc* Dunnett's test for parametric data sets and Kruskal-Wallis test with *post-hoc* Mann-Whitney pairwise comparison for non-parametric data sets. For all data sets, *p* values ≤ 0.05 were considered significant. Statistics employed in each experiment are also provided in the figure legends or in text. Statistical analyses were conducted with PAST (Paleontological Statistics Software) or SPSS16.0 (SPSS, Chicago, IL).

3. **Results**

3.1 Na$^+$ and ammonia flux pharmacological inhibition

Sodium uptake decreased in a dose-dependent manner with both increasing amiloride (>5 μmol l^{-1}) and EIPA (>1 μmol l^{-1}) concentrations to a maximal observed reduction of $47 \pm 13\%$ and $77.5 \pm 3\%$, respectively (Figs. 1A, 2A). Further, DAPI and phenamil reduced Na$^+$ uptake by $50 \pm 13.5\%$, and $73 \pm 9\%$, respectively (Fig. 3A). Inhibition of the VHA by KM91104 also decreased Na$^+$ uptake ($57 \pm 6\%$, Fig. 3A). The results from single pharmacological agent applications suggest that both Na$^+$ channels and NHEs function in epithelial Na$^+$ uptake. Therefore, to determine if one of these two transport mechanisms are more essential for epithelial Na$^+$ uptake, two to three inhibitors were combined for simultaneous exposure. Here, inhibitors were used to target the VHA mediated Na$^+$ channel mechanism (KM91104 + phenamil) alone and the VHA mediated Na$^+$ channel + NHE (KM91104 + phenamil + EIPA) mechanisms together. Disruption of the VHA mediated Na$^+$ channel mechanism alone decreased Na$^+$ uptake by $78 \pm 8\%$, while dual inhibition of VHA mediated Na$^+$ channel and NHE mechanisms reduced Na$^+$ uptake by $85 \pm 5\%$ (Fig. 3A). However, dual inhibition of VHA mediated Na$^+$ channel and NHE mechanisms did not cause significant reductions in Na$^+$ uptake compared to just inhibition of VHA mediated Na$^+$ channel mechanism or NHE mechanism alone.

Exposure of ETW acclimated leeches to exponentially increasing amiloride concentrations caused a maximum reduction in ammonia excretion rates by just $51 \pm 13.5\%$ at 500 μmol l^{-1}, with no inhibition at lower concentrations (Fig. 1B). In contrast, increasing concentrations ranging up to 100 μmol l^{-1} of the more specific NHE-inhibitor EIPA had no effect on ammonia excretion (Fig. 2B). Similar to EIPA, phenamil and DAPI had no effect on

ammonia excretion (Fig. 3B). However, inhibition of the VHA by KM91104 resulted in a 42 ± 10% decrease in ammonia excretion (Fig. 3B).

To determine whether environmental conditions unfavourable for electroneutral NHEs alter Na^+ and ammonia flux dynamics, pharmacological experiments performed on ETW acclimated leeches were repeated in low ionic strength water (0.05 mmol l^{-1} Na^+, pH 5) acclimated leeches. Here, all pharmacological agents were used at the same concentration as previous experiments and exhibited the same inhibitory effect on Na^+ uptake as well the lack of inhibition on ammonia excretion when compared to ETW acclimated leeches (Fig. 4).

3.2 Immunolocalization of vacuolar-type H^+-ATPase and Na^+/K^+-ATPase in leech skin

To determine the localization of the VHA and NKA within the skin of *N. obscura*, whole body sections were stained with anti-*VHA* (subunit B) or anti-*NKA* (α-subunit) antibodies. For anti-*VHA* sections, staining can be observed in the subcuticular layer, which is presumed to be the apical membrane of cutaneous epithelial cells (Fig. 5a, a′, d). VHA staining was not uniform across the surface of the skin but appeared restricted to the "pit" regions of leech skin folds (Fig. 5d). For anti-*NKA* sections, staining is present throughout the epithelial cell cytoplasm and in the basolateral membrane of epithelial cells (Fig. 5b, b′, d), which have extensive basolateral infoldings reaching up to 1 μm from the apical membrane (Blackshaw, 1981). Here, NKA staining signals do not reach the area of the apical membrane, where anti-*VHA* staining was observed (Fig. 5a′, b′). Unlike the VHA, NKA staining is uniform across the entire leech skin (Fig. 5e). Further, incubation of sections in null controls showed no background fluorescence (Fig. 5c,c′, f).

3.3 mRNA expression of Na$^+$ and ammonia transporters in the skin

Using degenerate primers, RT-PCR was preformed to confirm the presence of NHE and Na$^+$ channel like genes within the skin of leeches (Table 1). A partial sequence of the *N. obscura* NHE3-like and amiloride sensitive Na$^+$ channel-like genes were successfully amplified in the leech skin (GB Accession nos.:KY551583 and KY551584). BLASTx analysis of the *N. obscura* NHE-like gene demonstrated a 57 and 48% amino acid identity to the previously identified apical NHE3 in squid *Sepioteuthis lessoniana* and NHE in shore crab *Carcinus maenas*, respectively (Hu et al., 2014; Towle et al., 1997). Additionally, BLASTx analysis of the *N. obscura* putative Na$^+$ channel identified the nucleotide fragment as a member of the amiloride sensitive Na$^+$ channel superfamily, which contained a 70% identity to the leech *Helobdella robusta* putative amiloride sensitive Na$^+$ channel.

Quantitative PCR analysis showed that the transcript abundance of *NoNHE* was significantly higher (1.6-fold) in leeches exposed to low ionic strength water compared to those in ETW acclimated leeches (Fig. 6). Other measured genes including *NoNaC*, *NoRhp*, and *NoVHA* had no change in transcript abundance between low ionic strength and ETW acclimated leeches (Fig. 6).

3.4 pH and high environmental ammonia effects on Na$^+$ and ammonia flux

Exposure of leeches to varying unbuffered pH regimes ranging from 5 to 9.5 caused pH-dependent changes in ammonia excretion and Na$^+$ uptake (Fig. 7). Under control conditions (ETW, pH 8), the corresponding ammonia excretion and Na$^+$ uptake rates were 147 ± 18 nmol g^{-1} h^{-1} and 69 ± 14 nmol g^{-1} h^{-1}, respectively. Exposing leeches to pH 7 and 9.5 caused no changes to either ammonia excretion or Na$^+$ uptake. In contrast, at pH 6 Na$^+$ uptake rates increased while ammonia excretion rates remained unchanged relative to control

conditions (pH 8). At pH 5 ammonia excretion was observed to increase to[1] and Na$^+$ uptake was unchanged compared to control conditions.

Previous studies have shown that acute exposure to HEA causes an activation of ammonia excretion in *N. obscura* (Quijada-Rodriguez et al., 2015). To determine if stimulation of ammonia excretion alters Na$^+$ uptake, leeches were acutely (1 hour) exposed to HEA (1 mmol l^{-1} NH$_4$Cl, pH 8) and both Na$^+$ and ammonia flux rates were measured. Acute (1h) exposure of leeches to HEA resulted in the expected increase in ammonia excretion rates from 147 $\pm$ 18 nmol g^{-1} h^{-1} (ammonia free, pH 8) to 1030 $\pm$ 312 nmol g^{-1} h^{-1} (HEA, pH 8; Fig. 8B). In contrast, Na$^+$ uptake remained constant with HEA exposure (Fig. 8A). During HEA exposure it may be possible for other ammonia transporting tissues to contribute to the observed increases in ammonia excretion, therefore, flux rates of ammonia loaded leeches were measured to investigate the effect that cutaneous ammonia excretion may have on Na$^+$ uptake. Transferring ammonia loaded leeches (1 hour ammonia loading in HEA) to ammonia free water caused an approximately two-fold increase in ammonia excretion compared to control leeches, which was consequently coupled with a 0.6 fold decrease in Na$^+$ uptake (Fig. 8).

4. Discussion

The main objectives of the present study were to identify the mechanism of apical Na$^+$ uptake and its link to ammonia excretion across the skin of the freshwater ribbon leech *N. obscura*. This study provides strong physiological and molecular evidence for both Na$^+$ channel and NHE mediated Na$^+$ uptake mechanisms being present and functional in the skin of *N. obscura*. Additionally, Na$^+$ uptake and ammonia excretion over the apical membrane is not coupled, refuting a role for a NHE-Rh metabolon in *N. obscura* as a requirement for NHEs to overcome thermodynamic constraints poised by freshwater environments. However,

one caveat to interpretations of this study is that we assume specificity of the employed pharmacological agents based on documented effects on the respective counterpart transporters in vertebrates.

The results from pharmacological experiments suggest that *N. obscura* uses at least two mechanisms for Na^+ uptake. This is consistent with the observations of Sobczak and colleagues (2007), who suggested that two Na^+ uptake mechanisms exist in the skin of the medicinal leech *H. medicinalis*. This conclusion was made on the basis that the general Na^+ channel and NHE inhibitor, amiloride, only partially inhibited Na^+ uptake in the skin of the medicinal leeches (Sobczak et al., 2007). In the present study, similar results were observed when employing amiloride (Fig. 1); however, experiments in this study using more specific Na^+ transporter inhibitors (DAPI, phenamil, and EIPA) suggest amiloride may not be as effective at inhibiting Na^+ channels or NHEs and should, therefore, be used with caution in future studies assessing Na^+ transport mechanisms.

Recently, ASICs were identified in rainbow trout and zebrafish gills and demonstrated to be the possible candidate Na^+ channel responsible for apical Na^+ uptake coupled with VHA in freshwater fish gills (Dymowska et al., 2014; Dymowska et al., 2015). Additionally, Dymowska and colleagues (2014) demonstrated that the ASIC inhibitor DAPI was highly specific for Na^+ channels as it did not affect fish NHEs. Therefore, observed reductions in Na^+ uptake when employing DAPI (Fig. 3) in the current study may possibly be attributed to the presence of an ASIC-like Na^+ channel in the skin of *N. obscura*. This notion is further supported by the observed reduction in Na^+ uptake upon application of the ENaC and ASIC inhibitor phenamil (Fig. 3). The underlying problem with an ASIC Na^+ channel in invertebrates is that neither ASIC nor ENaC proteins have been identified at the molecular level in any invertebrate rendering an ASIC Na^+ channel in *N. obscura* improbable (Hanukoglu and Hanukoglu, 2016). However, numerous homologous proteins, which are

members of distinct Na^+ channel families within the ENaC/degenerin Na^+ channel superfamily, have been identified in invertebrates such as the FMRFamide activated Na^+ channels of molluscs, degenerins in nematodes, and Ripped pocket and Pickpocket Na^+ channels in *Drosophila* (Hanukoglu and Hanukoglu, 2016; Kellenberger and Schild, 2002). In this study, an mRNA transcript of a Na^+ channel within the ENaC/degenerin superfamily was identified in the skin of *N. obscura* (NoNac) and is speculated to be the candidate Na^+ channel inhibited by DAPI and phenamil.

As mentioned previously, apical Na^+ uptake in freshwater organisms through Na^+ channels is thought to be electrically coupled to a cellular hyperpolarization energized by an apical VHA. Indeed, experiments using KM91104 (Fig. 3) suggest that the VHA in *N. obscura* is indeed involved in apical Na^+ uptake. At least in zebrafish, ASIC Na^+ channels have been shown to be co-localized with the VHA in H^+-ATPase rich cells, supporting the hypothesis of a VHA-dependent Na^+ channel mechanism (Dymowska et al., 2015). However, the role of VHA in stimulating Na^+ uptake at least in ASIC-like transporters is debated as to whether the Na^+ channel is activated by extracellular H^+ or whether the voltage gradient created by H^+ extrusion drives uptake through the Na^+ channels into the epithelial cells (Dymowska et al., 2015). Nevertheless, in the current study the observed inhibition of Na^+ uptake by both phenamil and KM91104 (Fig. 3A) supports a VHA dependent Na^+ channel mechanism in the skin of *N. obscura*. Furthermore, when both inhibitors were combined together there was no additional effect on Na^+ uptake, indicating that either inhibitor alone is capable of maximally inhibiting the VHA-dependent Na^+ channel pathway.

Given the theoretical thermodynamic constraints of NHEs at extremely low environmental Na^+ concentrations and low pH (Parks et al., 2008), we measured changes in mRNA transcript abundance and employed pharmacological agents to determine if Na^+ uptake mechanisms changed following acclimation to these NHE "unfavourable" conditions.

Similar to NHE3 in trout, euryhaline pupfish and zebrafish larvae (Boyle et al., 2016; Brix et al., 2015; Shih et al., 2012), acclimation to very low Na^+ concentrations caused an increase in mRNA transcript abundance of the *N. obscura* NHE3-like gene, while transcript abundance of the Na^+ channel, VHA, and Rh proteins all remained unchanged (Fig. 6). The increase in transcript abundance only for the NHE potentially implies that in *N. obscura,* NHEs may become the more important mechanism at extremely low environmental Na^+ and that ammonia excretion may not be necessary to potentially facilitate NHE function. However, it should be noted that a substantial pH stress (pH 5) was also imposed together with the low environmental $[Na^+]$ and due to the role of NHEs in proton excretion the change in mRNA expression of the NHE gene may have been more heavily influenced by the pH stress.

When challenged with extremely low $[Na^+]$ and low environmental pH (0.05 mmol l^{-1}, pH 5), EIPA still caused a reduction in Na^+ uptake (Fig. 4), implying that NHEs remain functional and overcome thermodynamic constraints caused by low Na^+ and low pH environments. Contrary to mRNA expression data, inhibition of the VHA mediated Na^+ channel mechanism by either DAPI, phenamil and KM91104 demonstrated that Na^+ channels and the VHA remain important for apical Na^+ uptake (Fig. 4). While both mechanisms remain functional regardless of environmental Na^+ concentration, whether one mechanism is more dominant cannot be determined based on mRNA or pharmacological data alone, as triple inhibition of NHEs, VHA and Na^+ channels (phenamil+KM91104+EIPA) did not cause further reductions of Na^+ uptake when compared to just EIPA or phenamil and KM91104 combination (Fig. 3). Furthermore, no difference in inhibitory effect is evident when comparing reductions in Na^+ uptake when employing EIPA and phenamil together with KM91104 (Fig. 3).

Although Na^+ channels and NHEs could not be localized in this study, our immunofluorescence experiments showed that VHA is localized in pit regions of the skin at

the apical membrane of the epithelia in an irregular pattern (i.e. not present in all skin epithelial cells), while NKA was localized in the basolateral membrane of all skin epithelial cells (Fig. 5e). The disperse NKA staining may be attributed to extensive basolateral infoldings or association of a tubular system to basolateral membrane as seen in fish mitochondrion rich cells (Wilson and Laurent, 2002). The staining pattern of VHA compared to the NKA implies that leech skin contains different epithelial cell types, henceforth referred to as VHA$^+$ and VHA$^-$ cells. Based on localization of the VHA and identification of the importance of the VHA in ammonia excretion, one can assume that ammonia excretion occurs in the VHA$^+$-cell rich pit regions of the leech skin. While mainly speculative, one can predict based on evidence from pharmacological experiments in this study and Na$^+$ channel localization relative to VHA in zebrafish gills (Dymowska et al., 2015) that the Na$^+$ channel in *N. obscura* is likely localized to the VHA$^+$ cells. In contrast, predications cannot be made on whether VHA$^+$ or VHA$^-$ cells of *N. obscura* contain NHEs. In the zebrafish H$^+$-ATPase rich cells the VHA, Na$^+$ channel, and NHE are all expressed in this single cell type, however, in rainbow trout PNA$^+$ cells express NHEs whereas PNA$^-$ cells express the VHA and Na$^+$ channels (Dymowska et al., 2012; Dymowska et al., 2014; Hwang et al., 2011). Therefore, further immunolocalization studies are required to identify the cell types and transporters present in each cell type to make more informed conclusions on Na$^+$ uptake mechanisms.

As mentioned in the introduction, Na$^+$ uptake can be linked to ammonia excretion in some freshwater species via the NHE-Rh metabolon hypothesized by Wright and Wood (2009). In zebrafish larvae, where an NHE-Rh metabolon has been suggested, inhibition of NHEs by EIPA caused reduced Na$^+$ uptake, ammonia excretion, and proton excretion (Shih et al., 2012). However, for *N. obscura* in both low Na$^+$ (0.45 mmol l^{-1}) and extremely low Na$^+$ (0.05 mmol l^{-1}) EIPA only caused decreased Na$^+$ uptake and did not alter ammonia excretion, indicating that NH$_3$ molecules passing through apical Rh proteins are not

generating localized alkalization to facilitate NHE function in low Na^+ environments. An ammonia independent Na^+ uptake by NHEs is further supported by mRNA expression experiments, where acclimation to extremely low $[Na^+]$ led to an upregulation of the *N. obscura* NHE3-like gene while mRNA transcript abundance of the Rh protein was unaltered. This is contrary to what has been previously observed in freshwater fish, where an NHE-Rh metabolon is proposed (Shih et al., 2012; Wu et al., 2010).

The effects of amiloride on both Na^+ uptake and ammonia excretion across the leech skin at higher concentrations (500 μmol l^{-1} amiloride) were conflicting to the ammonia independent Na^+ uptake theory. However, the lack of effect on ammonia excretion when employing EIPA, DAPI and phenamil suggests that the observed decrease in ammonia excretion by amiloride is likely not linked to inhibition of Na^+ channels or NHEs. It has been previously shown that amiloride reduces cAMP accumulation in trout erythrocytes at inhibitory concentrations used in this study (Mahe et al., 1985). Therefore, the lack of specificity by amiloride suggests the effect on ammonia excretion observed in this study maybe due to an alternative effect to the ammonia excretion machinery and not a direct effect on Na^+ channels or NHEs.

Previous studies on *N. obscura* revealed that ammonia excretion could be stimulated by decreasing pH and exposing leeches to high environmental ammonia (Quijada-Rodriguez et al., 2015). When exposed to decreasing pH levels, ammonia excretion continually increased and Na^+ uptake rates increased up until pH 6 and then began decreasing (Fig. 7). Clearly, this implies that Na^+ uptake is not dependent on ammonia excretion as increased ammonia excretion does not necessarily correlate to increased Na^+ uptake as would be expected in an ammonia dependent Na^+ uptake mechanism. Further, high environmental ammonia (HEA) exposure and post-HEA (ammonia loaded leeches) experiments further

confirm an ammonia independent Na^+ uptake theory for *N. obscura* as increasing ammonia excretion under both of these treatments did not stimulate Na^+ uptake (Fig. 8).

Although Na^+ channels and NHEs do not link Na^+ uptake and ammonia excretion, based on the results of fluxes employing KM91104, VHA appears to be involved in both Na^+ uptake and ammonia excretion (Fig. 3). In a previous study on ammonia excretion in *N. obscura*, we demonstrated that VHA may be involved in ammonia excretion by stimulating acid trapping of ammonia (Quijada-Rodriguez., 2017; Quijada-Rodriguez et al., 2015), a phenomenon previously described in the freshwater planarian *Schmidtea mediterranea* (Quijada-Rodriguez et al., 2017; Weihrauch et al., 2012). This occurs via the acidification of the boundary layer by the VHA on the epithelial cell surface of the skin creating a partial pressure gradient that drives NH_3 excretion by Rh proteins (Quijada-Rodriguez et al., 2017; Weihrauch et al., 2012). Since the acid trapping mechanism of ammonia excretion is independent of apical Na^+ transporters and ammonia excretion was shown in this study to not directly couple to Na^+ uptake, it is likely that ammonia excretion and Na^+ uptake are both dependent on VHA mediated proton excretion but not directly dependent on one another.

Clearly, the results of this study suggest NHEs in *N. obscura* are functional in dilute freshwater even though an NHE-Rh metabolon is not present. Potential alternatives theories to facilitate NHE function in thermodynamically unfavourable dilute freshwater may include a carbonic anhydrase (CA) assisted NHE mechanism, a low intracellular Na^+ microenvironment created by NKA, and electrogenic NHEs. In euryhaline pupfish and white sturgeon where a CA assisted NHE mechanism has been proposed, CA mediated CO_2 hydration is thought to generate increased intracellular H^+ concentration, which drives H^+ excretion by NHEs and facilitates Na^+ uptake (Brix et al., 2015; Shartau et al., 2017). However, it is unlikely that CA mediated CO_2 hydration alone would provide sufficient increases in intracellular H^+ concentration to allow proper NHE function in acidic freshwater

environments where inwardly directed H^+ gradients would be highly favoured. Alternatively, NKA in the basolateral infoldings may contribute to facilitating NHE function by creating low intracellular Na^+ microenvironments below the apical membrane surface (Kumai and Perry, 2012). In leeches, electron microscopy images of the skin epithelia indicate that the basolateral membrane contains many infoldings that reach as close as 1 μm from the apical surface (Blackshaw, 1981), which could potentially position the NKA close enough to apical membranes to generate low intracellular Na^+ microenvironments below the apical membrane. Immunolocalization of NKA in this study further supports a potential low intracellular Na^+ micrenvironment as staining signal shows that NKA can be found very close to the apical membrane (Fig. 5). Another alternative for facilitated NHE function proposed by Clauss (2001) and based on unpublished results, is an electrogenic NHE (i.e. $2Na^+/1H^+$ exchange). In this model, the electrogenic Na^+ uptake by NHEs in leech skin may be similar to electrogenic NHEs described in crustacean gills and hepatopancreas (Ahearn et al., 2001; Towle, 1989). While no follow up studies on the electrogenic Na^+ uptake by leech skin have focused on electrogenic NHE theory, we hypothesize that an electrogenic NHE maybe present in the skin of *N. obscura* as a mechanism to facilitate Na^+ uptake. An electrogenic NHE would reduce thermodynamic constraints on NHEs, as it would not be driven only by chemical gradients but also electrical gradients such as that provided by an apical VHA. This would allow changes in cell potential to stimulate Na^+ uptake. Whether either of the three or a combination of aforementioned alternatives are present remain speculative at the moment and require further studies to clarify the phenomena of Na^+ uptake by NHEs in *N. obscura* inhabiting dilute freshwater.

In conclusion, we have demonstrated through physiological and molecular experiments that *N. obscura* likely employs both, an NaC-VHA and NHE based Na^+ uptake mechanisms, where both mechanisms may or may not be located in the same epithelial cell

type. Furthermore, we determined that under extremely low environmental Na$^+$ (0.05 mmol l^{-1}, pH 5), Na$^+$ uptake remained sensitive to inhibition of VHA dependent Na$^+$ channel and NHE mechanisms; however, we are unable to conclude whether additional mechanisms such as, Na$^+$/Cl$^-$ cotransporters as have been found in zebrafish (Wang et al., 2009) are present. Additionally, we concluded that Na$^+$ uptake and ammonia excretion are uncoupled in *N. obscura* and therefore, an NHE-Rh metabolon does not explain the thermodynamic phenomena of functional NHEs in freshwater for *N. obscura*. Instead we postulate the idea of NHEs overcoming thermodynamic constraints through a CA assisted NHE mechanism, Na$^+$/K$^+$ ATPase generated low intracellular Na$^+$ microenvironment below the apical membrane and electrogenic NHEs for apical Na$^+$ uptake in freshwater environments.

Acknowledgements

Competing interests

The authors declare no competing, financial or otherwise conflicts of interest

Author contributions

A.R.Q-R., A.G.S., G.G.G., and D.W. conceptualized and designed the research. A.R.Q-R, A.G.S., J.M.W., Y.H., and G.J.P.A. performed experiments and analyzed the data. A.R.Q-R., A.G.S., G.G.G., and D.W. interpreted the results of the experiments. A.R.Q-R. and J.M.W prepared the figures. A.R.Q-R. drafted the manuscript. All authors revised and edited the final manuscript.

Funding

References

Ahearn, G. A., Mandal, P. K. and Mandal, A. (2001). Biology of the 2Na$^+$/1H$^+$ Antiporter in Invertebrates. *J. Exp. Zool.* **289**, 232–244.

Avella, M. and Bornancin, M. (1989). A new analysis of ammonia and sodium transport through the gills of the freshwater rainbow trout (Salmo gairdneri). *J. Exp. Biol.* **142**, 155–175.

Blackshaw, S. E. (1981). Morphology and distribution of touch cell terminals in the skin of the leech. *J. Physiol.* **320**, 219–228.

Boyle, D., Blair, S. D., Chamot, D. and Goss, G. G. (2016). Characterization of developmental Na(+) uptake in rainbow trout larvae supports a significant role for Nhe3b. *Comp. Biochem. Physiol. A. Mol. Integr. Physiol.* **201**, 30–36.

Brix, K. V, Esbaugh, A. J., Mager, E. M. and Grosell, M. (2015). Comparative evaluation of Na(+) uptake in Cyprinodon variegatus variegatus (Lacepede) and Cyprinodon variegatus hubbsi (Carr) (Cyprinodontiformes, Teleostei): Evaluation of NHE function in high and low Na(+) freshwater. *Comp. Biochem. Physiol. A. Mol. Integr. Physiol.* **185**, 115–124.

Chen, X., Qiu, L., Li, M., Dürrnagel, S., Orser, B. A., Xiong, G. and MacDonald, J. F. (2010). Diarylamidines: High potency inhibitors of acid-sensing ion channels. *Neuropharmacology* **58**, 1–22.

Clauss, W. G. (2001). Epithelial transport and osmoregulation in annelids. *Can. J. Zool.* **79**, 192–203.

Davies, R. W. (1973). The geographic distribution of freshwater Hirudinoidea in Canada. *Can. J. Zool.* **51**, 531–545.

Dymowska, A. K., Hwang, P.-P. and Goss, G. G. (2012). Structure and function of ionocytes in the freshwater fish gill. *Respir. Physiol. Neurobiol.* **184**, 282–292.

Dymowska, A. K., Schultz, A. G., Blair, S. D., Chamot, D. and Goss, G. G. (2014). Acid-sensing ion channels are involved in epithelial Na$^+$ uptake in the rainbow trout Oncorhynchus mykiss. *Am. J. Physiol. Cell Physiol.* **307**, C255–65.

Dymowska, A. K., Boyle, D., Schultz, A. G. and Goss, G. G. (2015). The role of acid-sensing ion channels in epithelial Na$^+$ uptake in adult zebrafish (Danio rerio). *J. Exp. Biol.* **218**, 1244–51.

Edwards, S. L., Tse, C. M. and Toop, T. (1999). Immunolocalisation of NHE3-like immunoreactivity in the gills of the rainbow trout (Oncorhynchus mykiss) and the blue-throated wrasse (Pseudolabrus tetrious). *J. Anat.* **195**, 465–469.

Esaki, M., Hoshijima, K., Kobayashi, S., Fukuda, H., Kawakami, K. and Hirose, S. (2007). Visualization in zebrafish larvae of Na$^+$ uptake in mitochondria-rich cells whose differentiation is dependent on foxi3a. *Am. J. Physiol. - Regul. Integr. Comp. Physiol.* **292**, R470–R480.

Fehsenfeld, S. and Weihrauch, D. (2016). Mechanisms of acid – base regulation in seawater-acclimated green crabs (Carcinus maenas). *Can. J. Zool.* **94**, 95–107.

Fenwick, J. C., Bonga, S. E. W. and Flik, G. (1999). In vivo bafilomycin-sensitive Na$^+$ uptake in young freshwater fish. *J. Exp. Biol.* **202**, 3659–3666.

Genz, J., Carriere, B. and Anderson, W. G. (2013). Mechanisms of calcium absorption by anterior and posterior segments of the intestinal tract of juvenile lake sturgeon. *Comp. Biochem. Physiol. A. Mol. Integr. Physiol.* **166**, 293–301.

Goss, G. G. and Wood, C. M. (1990). Na$^+$ and Cl$^-$ uptake kinetics, diffusive effluxes and acidic equivalent fluxes across the fills of rainbow trout I. Response to environmental hyperoxia. *J. Exp. Biol.* **152**, 521–547.

Hanukoglu, I. and Hanukoglu, A. (2016). Epithelial sodium channel (ENaC) family: Phylogeny, structure-function, tissue distribution, and associated inherited diseases. *Gene* **579**, 95–132.

Hirata, T., Kaneko, T., Ono, T., Nakazato, T., Furukawa, N., Hasegawa, S., Wakabayashi, S., Shigekawa, M., Chang, M.-H., Romero, M. F., et al. (2003). Mechanism of acid adaptation of a fish living in a pH 3.5 lake. *Am. J. Physiol. - Regul. Integr. Comp. Physiol.* **284**, R1199–R1212.

Horng, J.-L., Lin, L.-Y., Huang, C.-J., Katoh, F., Kaneko, T. and Hwang, P.-P. (2007). Knockdown of V-ATPase subunit A (atp6v1a) impairs acid secretion and ion balance in zebrafish (Danio rerio). *Am. J. Physiol. Regul. Integr. Comp. Physiol.* **292**, R2068–2076.

Hu, M. Y., Guh, Y.-J., Stumpp, M., Lee, J.-R., Chen, R.-D., Sung, P.-H., Chen, Y.-C., Hwang, P.-P. and Tseng, Y.-C. (2014). Branchial NH_4^+-dependent acid–base transport mechanisms and energy metabolism of squid (Sepioteuthis lessoniana) affected by seawater acidification. *Front. Zool.* **11**, 55.

Hwang, P.-P. (2009). Ion uptake and acid secretion in zebrafish (Danio rerio). *J. Exp. Biol.* **212**, 1745–52.

Hwang, P.-P., Lee, T.-H. and Lin, L.-Y. (2011). Ion regulation in fish gills: recent progress in the cellular and molecular mechanisms. *Am. J. Physiol. Regul. Integr. Comp. Physiol.* **301**, R28–47.

Inokuchi, M., Hiroi, J., Watanabe, S., Hwang, P.-P. and Kaneko, T. (2009). Morphological and functional classification of ion-absorbing mitochondria-rich cells in the gills of Mozambique tilapia. *J. Exp. Biol.* **212**, 1003–10.

Ivanis, G., Esbaugh, a J. and Perry, S. F. (2008). Branchial expression and localization of SLC9A2 and SLC9A3 sodium/hydrogen exchangers and their possible role in acid-base regulation in freshwater rainbow trout (Oncorhynchus mykiss). *J. Exp. Biol.* **211**, 2467–77.

Kartner, N., Yao, Y., Li, K., Crasto, G. J., Datti, A. and Manolson, M. F. (2010). Inhibition of osteoclast bone resorption by disrupting vacuolar H^+-ATPase a3-B2 subunit interaction. *J. Biol. Chem.* **285**, 37476–90.

Kellenberger, S. and Schild, L. (2002). Epithelial sodium channel / degenerin family of ion channels : A variety of functions for a shared structure. 735–767.

Kleyman, T. R. and Cragoe, E. J. (1988). Amiloride and its analogs as tools in the study of ion transport. *J. Membr. Biol.* **105**, 1–21.

Kumai, Y. and Perry, S. F. (2011). Ammonia excretion via Rhcg1 facilitates Na^+ uptake in larval zebrafish, Danio rerio, in acidic water. *Am. J. Physiol. Regul. Integr. Comp. Physiol.* **301**, R1517–R1528.

Kumai, Y. and Perry, S. F. (2012). Mechanisms and regulation of Na(+) uptake by freshwater fish. *Respir. Physiol. Neurobiol.* **184**, 249–56.

Larsen, E. H., Deaton, L. E., Onken, H., O'Donnell, M., Grosell, M., Dantzler, W. H. and Weihrauch, D. (2014). Osmoregulation and excretion. *Compr. Physiol.* **4**, 405–573.

Mahe, Y., Garcia-Romeu, F. and Motais, R. (1985). Inhibition by amiloride of both adenylate cyclase activity and the Na^+/H^+ antiporter in fish erythrocytes. *Eur. J. Pharmacol.* **116**, 199–206.

Parks, S. K., Tresguerres, M. and Goss, G. G. (2008). Theoretical considerations underlying Na(+) uptake mechanisms in freshwater fishes. *Comp. Biochem. Physiol. C. Toxicol. Pharmacol.* **148**, 411–418.

Quijada-Rodriguez, A. R., Treberg, J. R. and Weihrauch, D. (2015). Mechanism of ammonia excretion in the freshwater leech Nephelopsis obscura: characterization of a primitive Rh protein and effects of high environmental ammonia. *Am. J. Physiol. Regul. Integr. Comp. Physiol.* **309**, R692–705.

Shartau, R. B., Brix, K. V and Brauner, C. J. (2017). Characterization of Na(+) transport to gain insight into the mechanism of acid-base and ion regulation in white sturgeon (Acipenser transmontanus). *Comp. Biochem. Physiol. A. Mol. Integr. Physiol.* **204**, 197–204.

Shih, T.-H., Horng, J.-L., Liu, S.-T., Hwang, P.-P. and Lin, L.-Y. (2012). Rhcg1 and NHE3b are involved in ammonium-dependent sodium uptake by zebrafish larvae acclimated to low-sodium water. *Am. J. Physiol. Regul. Integr. Comp. Physiol.* **302**, R84–93.

Sobczak, K., Willing, A., Kusche, K., Bangel, N. and Weber, W.-M. (2007). Amiloride-sensitive sodium absorption is different in vertebrates and invertebrates. *Am. J. Physiol. Regul. Integr. Comp. Physiol.* **292**, R2318–27.

Towle, W. (1989). Electrogenic sodium-proton exchange in membrane vesicles from crab (Carcinus maenas) gill. *Am. J. Physiol. - Regul. Integr. Comp. Physiol.* **26**, R924–R931.

Towle, D. W., Rushton, M. E., Heidysch, D., Magnani, J. J., Rose, M. J., Amstutz, A., Jordan, M. K., Shearer, D. W. and Wu, W. (1997). Sodium/proton antiporter in the euryhaline crab Carcinus maenas: molecular cloning, expression adn tissue distribution. *J. Exp. Biol.* **200**, 1003–1014.

Verdouw, H., Echteld, C. J. A. V. A. N. and Dekkers, E. M. (1977). Ammonia determination based on indophenol formation with sodium salicylate. *Water Res.* **12**, 399–402.

Wang, Y.-F., Tseng, Y.-C., Yan, J.-J., Hiroi, J. and Hwang, P.-P. (2009). Role of SLC12A10.2, a Na-Cl cotransporter-like protein, in a Cl uptake mechanism in zebrafish (Danio rerio). *Am. J. Physiol. Regul. Integr. Comp. Physiol.* **296**, R1650–60.

Weber, W., Dannenmaier, B. and Clauss, W. (1993). Ion transport across leech integument I. Electrogenic Na$^+$ transport and current fluctuation analysis of the apical Na+ channel. *J. Comp. Physiol. B Biochem. Syst. Environ. Physiol.* **163**, 153–159.

Weihrauch, D., Chan, A. C., Meyer, H., Döring, C., Sourial, M. and O'Donnell, M. J. (2012). Ammonia excretion in the freshwater planarian Schmidtea mediterranea. *J. Exp. Biol.* **215**, 3242–53.

Wilson, J. M., Laurent, P., Tufts, B. L., Benos, D. J., Donowitz, M., Vogl, A. W. and Randall, D. J. (2000). NaCl uptake by the branchial epithelium in freshwater teleost fish: An immunological approach to ion-transport protein localization. *J. Exp. Biol.* **203**, 2279–2296.

Wilson, J. M., Leitão, A., Gonçalves, A. F., Ferreira, C., Reis-Santos, P., Fonseca, A.-V., da Silva, J. M., Antunes, J. C., Pereira-Wilson, C. and Coimbra, J. (2007). Modulation of branchial ion transport protein expression by salinity in glass eels (Anguilla anguilla L.). *Mar. Biol.* **151**, 1633–1645.

Wright, P. A. and Wood, C. M. (2009). A new paradigm for ammonia excretion in aquatic animals: role of Rhesus (Rh) glycoproteins. *J. Exp. Biol.* **212**, 2303–2312.

Wu, S.-C., Horng, J.-L., Liu, S.-T., Hwang, P.-P., Wen, Z.-H., Lin, C.-S. and Lin, L.-Y. (2010). Ammonium-dependent sodium uptake in mitochondrion-rich cells of medaka (Oryzias latipes) larvae. *Am. J. Physiol. Cell Physiol.* **298**, C237–50.

Yan, J., Chou, M., Kaneko, T. and Hwang, P. (2007). Gene expression of Na$^+$/H$^+$ exchanger in zebrafish H$^+$-ATPase-rich cells during acclimation to low-Na$^+$ and acidic environments. *Am. J. Physiol. Cell Physiol.* **293**, C1814–C1823.
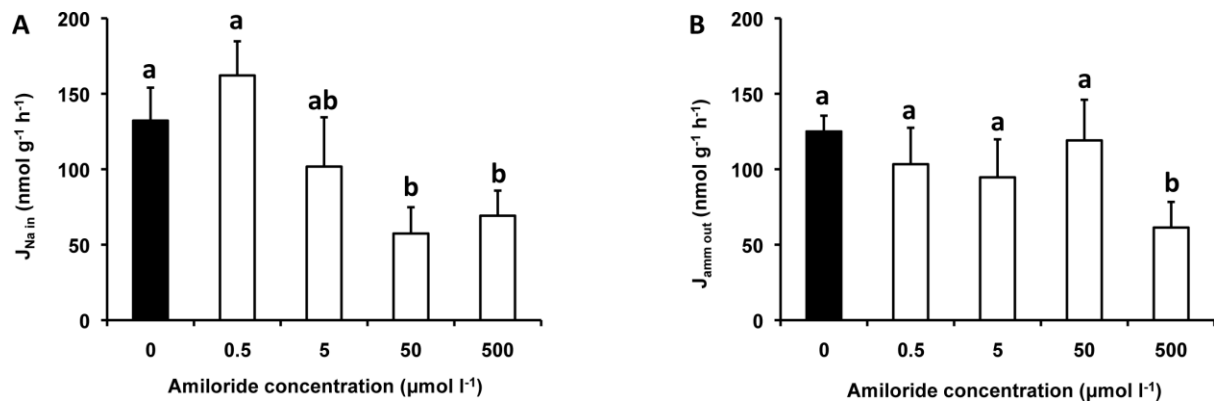
Figures

Figure 1. **The effect of amiloride on (A) Na$^+$ uptake and (B) ammonia excretion rates in** *Nephelopsis obscura* **acclimated to Edmonton tap water (0.45 mmol l^{-1} Na$^+$, pH 8).** Data are presented as mean ± s.e.m (n = 5-12). Means with the same letter are not significantly different from each other (one way ANOVA post-hoc Dunnett's test; $p \leq 0.05$).
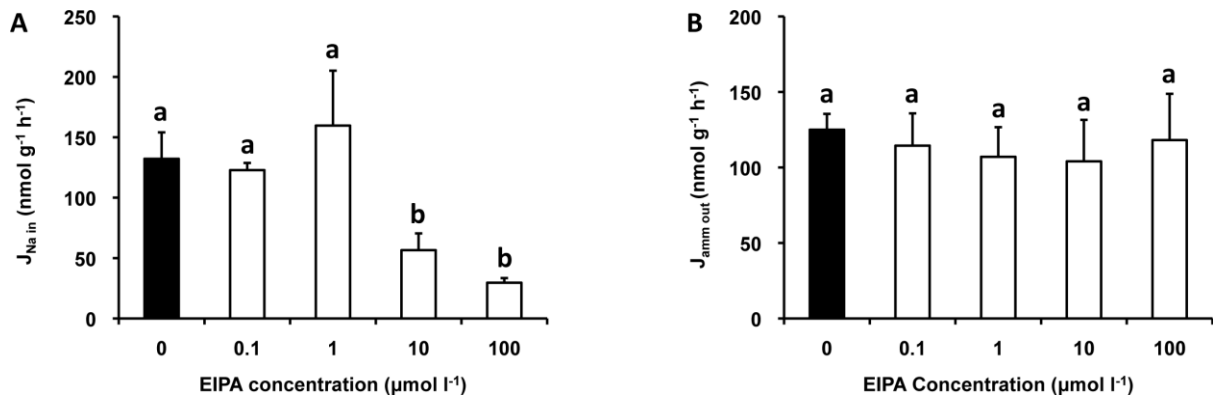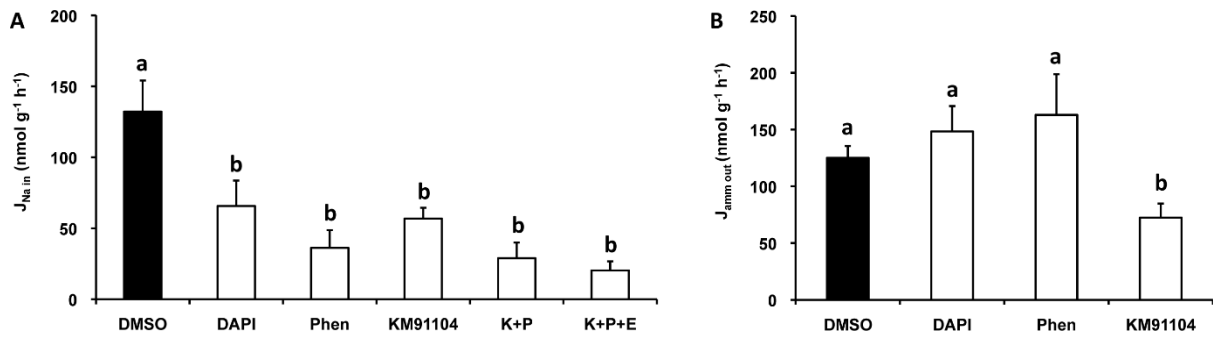
Figure 2. **The effect of EIPA on (A) Na$^+$ uptake and (B) ammonia excretion rates in *Nephelopsis obscura* acclimated to Edmonton tap water (0.45 mmol l^{-1} Na$^+$, pH 8).** Data are presented as mean ± s.e.m (n = 5-12). Means with the same letter are not significantly different from each other (one way ANOVA post-hoc Dunnett's test; *p ≤ 0.05*).

Figure 3. **The effect of DAPI, phenamil, and KM91104 on (A) Na$^+$ uptake and (B) ammonia excretion rates in *Nephelopsis obscura* acclimated to Edmonton tap water (0.45 mmol l^{-1} Na$^+$, pH 8).** K+P denotes treatment with KM91104 and phenamil together. K+P+E denotes treatment with KM91104, phenamil, and EIPA together. Data are presented as mean ± s.e.m (n = 6-12). Means with the same letter are not significantly different from each other (one way ANOVA post-hoc Dunnett's test; $p \leq 0.05$).
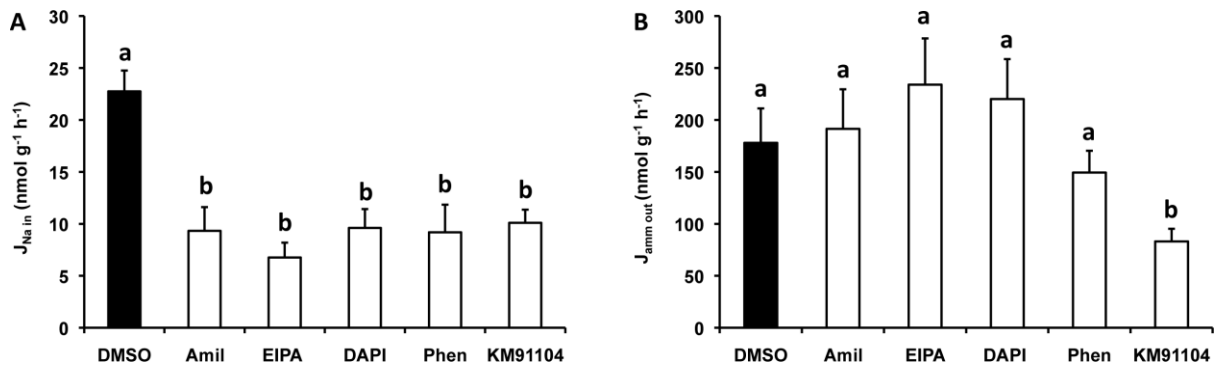
Figure 4. **The effect of amiloride, EIPA, DAPI, phenamil, and KM91104 on (A) Na$^+$ uptake and (B) ammonia excretion rates in** *Nephelopsis obscura* **acclimated to low ionic strength water (0.05 mmol l^{-1} Na$^+$, pH 5).** Data are presented as mean ± s.e.m (n = 6-12). Means with the same letter are not significantly different from each other (one way ANOVA post-hoc Dunnett's test; *p ≤ 0.05*).
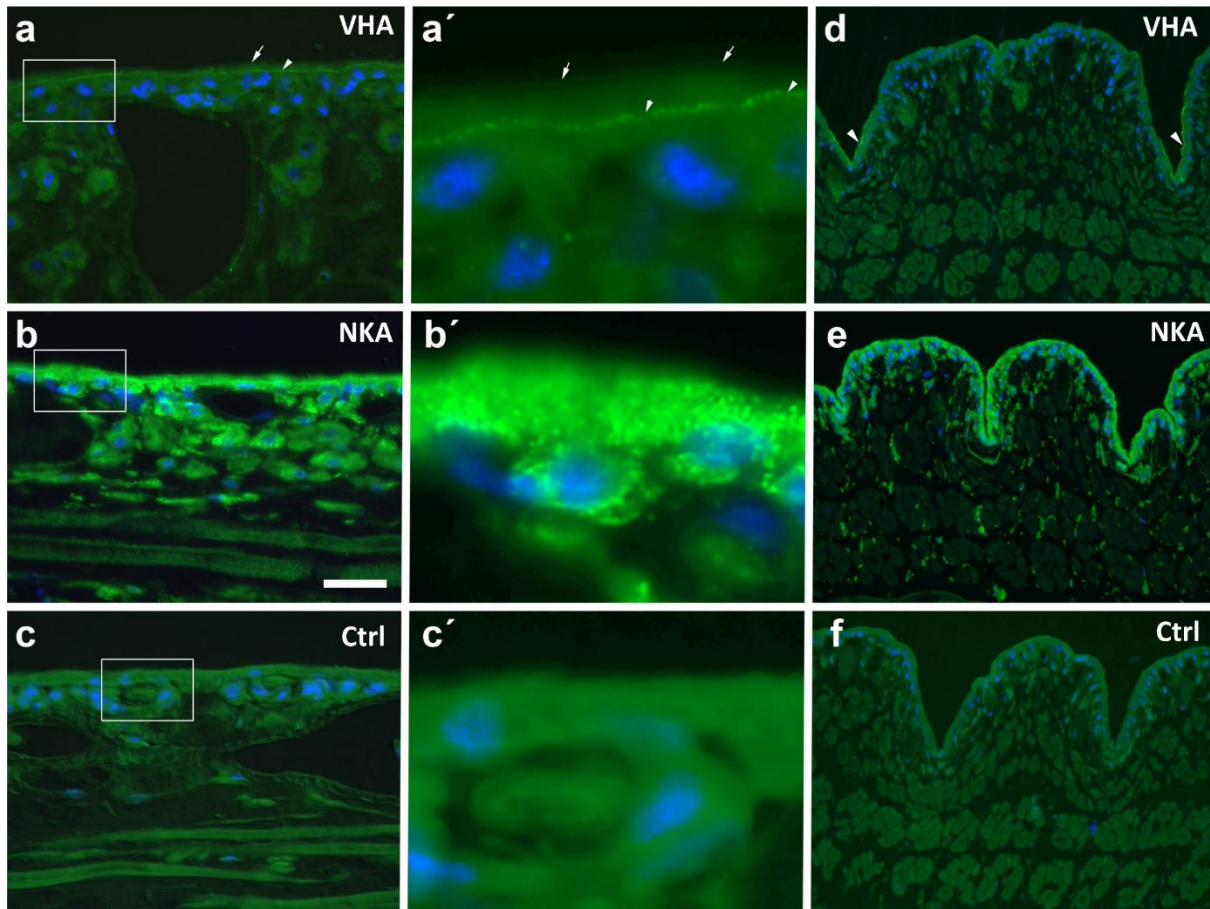
Figure 5. **Indirect immunofluorescence localization of (a,d) VHA and (b,e) NKA in dilute freshwater acclimated *Nephelopsis obscura*.** Normal rabbit serum negative control sections are also included (c,f) . High magnification insets are shown in a´, b´and c´, respectively. Sections are counter-stained with the nuclear stain DAPI and overlaid onto the corresponding differential interference contrast (DIC) images. Scale bar (a-c) 25 µm, (a´-c´) 5 µm or (d-f) 50 µm. Full white arrows indicate the leech skin cuticle and white arrow heads indicate the apical membrane of the epithelial cells.
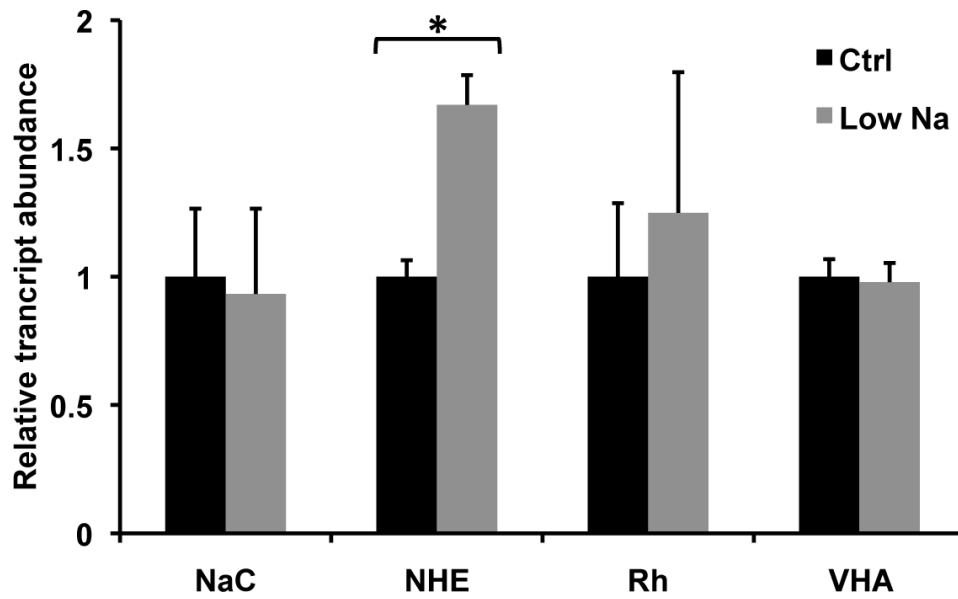
Figure 6. **Quantitative PCR analysis of Na$^+$ channel (NaC), Na$^+$/H$^+$ exchange 3 like (NHE), Rh protein (Rh), and vacuolar H$^+$-ATPase subunit B (VHA) genes from the skin of *Nephelopsis obscura* acclimated to Edmonton tap water and low ionic strength water.** Transcript abundance levels were normalized using the ribosomal protein S2 gene. Data are presented as mean ± s.e.m (n = 5-6). * indicates significant differences from Edmonton tap water acclimated leeches (Mann-Whitney U test; $p \leq 0.05$).
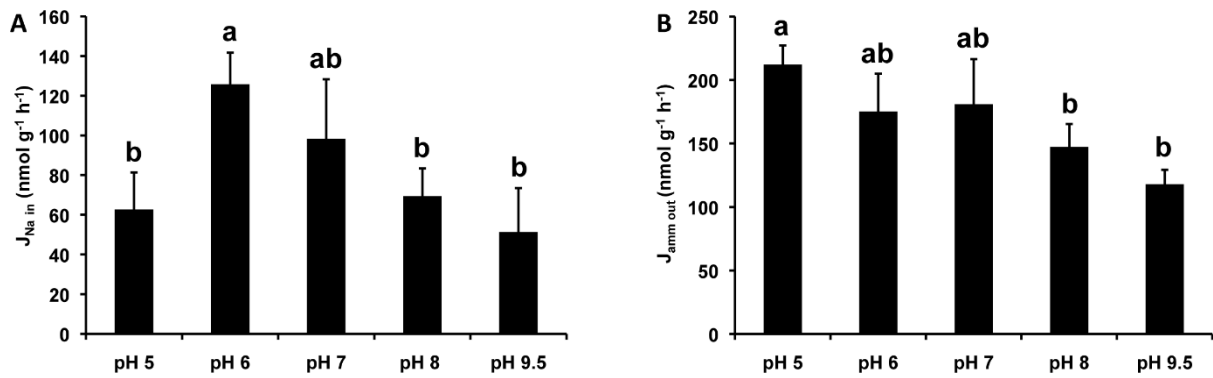
Figure 7. **The effect of pH on (A) Na$^+$ uptake and (B) ammonia excretion rates in** *Nephelopsis obscura* **acclimated to Edmonton tap water (0.45 mmol l^{-1} Na$^+$, pH 8).** Data are presented as mean ± s.e.m (n = 5-7). Means with the same letter are not significantly different from each other (Kruskal-Wallis test with *post hoc* Mann-Whitney U pairwise comparison; $p \leq 0.05$).
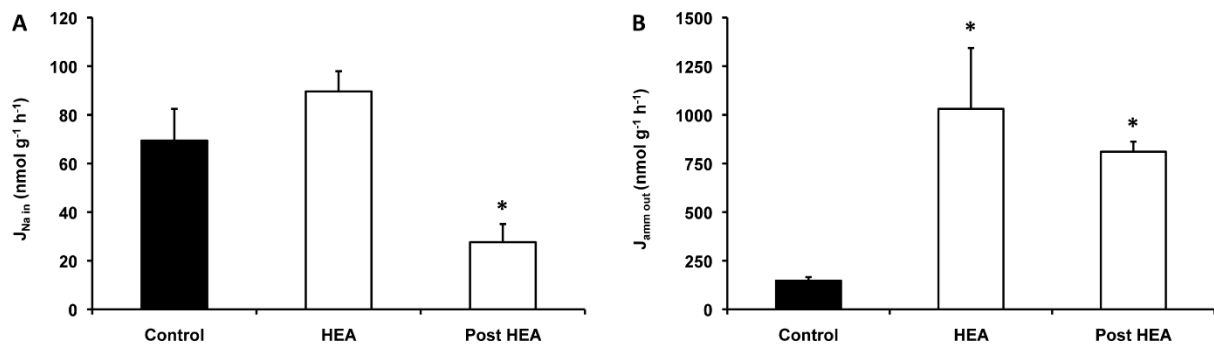
Figure 8. **The effect of high environmental ammonia (HEA) and ammonia loading (post-HEA) on (A) Na$^+$ uptake and (B) ammonia excretion rates in *Nephelopsis obscura* acclimated to Edmonton tap water (0.45 mmol l^{-1} Na$^+$, pH 8).** Data are presented as mean ± s.e.m (n = 6-11). * indicates significant differences from DMSO controls (Mann-Whitney U test; *p ≤ 0.05*).

Table 1. Degenerate and *Nephelopsis obscura* specific primers employed in RT-PCR.

Primer	Nucleotide sequence (5' → 3')	Annealing temp. (ºC)	Product size(bp)	Accession No.
NoRPS2 F1	GGGCGTTAAGTGCTCAAAAG	60	200	KM923910.1
NoRPS2 R1	CAACGATGCCAGTTCCTCTT	60		
DegNHE3 F	CCNCCATGCATCNTGGANGCAGCTTA	50	887	N/A
DegNHE3 R	CCTCCGTAAGCCATGATNAANTGTTC	50		
DegNaC F	ATGCCYTTYCCNGAMGGAYGARGG	45	200	N/A
DegNaC R	CANGTCTANWNACANCCYTTNTNRCARTA	45		
NoNaC RACE R1	AGTACTCGTTGTCGGATTCATG	60	N/A	N/A

N, replaces A/T/G/C; Y, replace C/T; M, replace A/C; R, replace A/G; W, replace A/T

Table 2. *Nephelopsis obscura* specific primers employ in quantitative PCR.

Primer	Nucleotide sequence (5' → 3')	Annealing temp. (ºC)	Product size(bp)	Efficency	Accession No.
NoRhp F	AGCCTGTTTGGAGGAGTTATC	60			
NoRhp R	CACCCAGTAATCCCAGTCATC	60	99	2.04	KM923907.1
NoVHA F	CATCACTCCTCGAATAGCTCTAAC	60			
NoVHA R	CTCTCTCAAAGCCTCAGCATAC	60	112	1.97	KM923908.1
NoNHE3 F	GCCATTCTCTCCTTGTCCTATG	60			
NoNHE3 R	GCCACATCCAATCATGCTTATG	60	84	2.04	KY551583
NoNaC F	CATTCAAGGCTGGTCCTAGATAC	60			
NoNaC R	GGAGACCAGCTGATTGAGTTATT	60	93	1.94	KY551584
NoRPS2 F2	GCTGTGGTAGTGTAGAAGTGAG	60			
No RPS2 R2	CAATTCCAGCCATGTGAAGAAG	60	99	1.94	KM923910.1